



3-5-8

PROPOSAL OF A MATHEMATICAL MODEL FOR EARTHQUAKE RESPONSE ANALYSIS OF IRREGULARLY BOUNDED SURFACE LAYER

Choshiro TAMURA¹ and Takeyasu SUZUKI²

¹Institute of Industrial Science, University of Tokyo
Minato-ku, Tokyo, Japan

²Institute of Construction Technology, Kumagai-gumi Co., Ltd.
Shinjuku-ku, Tokyo, Japan

SUMMARY

For earthquake response analysis of a soft surface layer which is not considered to be uniform in a three-dimensional expanse, a quasi-three dimensional ground model is proposed for practical use. Vibration model tests are carried out to examine the verification of the model. The new model is a kind of composite system of a lumped mass-spring system and two-dimensional FEM.

INTRODUCTION

Studies of interactions between underground structures and surrounding ground have included those by Dr. Okamoto on mountain tunnels (1948, 1963), Dr. Housner on BART tunnels, Dr. Sakurai on ground surface observations of pipelines (1967), Dr. Tajimi on dynamic analyses of foundations (1969), and Tamura proposing an analysis model for tunnels (1975). Subsequently, there have been many studies carried out, and differing from structures in the open air, it has come to be considered that, as a measure of the seismic force acting on an underground structure, the displacement during earthquake of the surrounding ground has been considered appropriate for evaluation of the earthquake resistance. This has been backed up by earthquake observations made on actual structures.

It has been recognized that in case there is a large difference in wave impedances between the surface layer ground and its basement, the influence of the profile of the surface layer on earthquake motion is substantial, and in aseismic analysis it is important for the behavior of the surface layer during earthquake to be investigated. The mathematical model previously proposed by Tamura determines earthquake response of the surface layer ground grasping the variation in the surface layer two-dimensionally (length in horizontal direction and depth). However, it is imaginable that the behavior of the surface layer ground will be extremely complex in case the ground condition changed sharply in a three-dimensional expanse. In this case, FEM is normally used for the three-dimensional study of the dynamic behavior of the surface layer ground in a broad area and in such case the relationship to be solved contains a very large number of unknowns so that the numerical calculations are actually close to impossible, and are not practical.

Therefore, the mathematical model previously proposed was extended and a quasi-three-dimensional mathematical model that could be applied to three dimensions was made up. It consists of the following main points:

- A. The surface layer ground is divided into vertical soil-column elements.

B. The soil-column elements are replaced by one-lumped-mass-spring systems that show shear vibrations.

C. The soil-column elements are transformed into plate elements, and spring constants for relative displacements between mass points are computed from these plate elements.

Employment of FEM will be convenient in computation of spring constants between mass points. The new model can be said to be a hybrid system of a lumped mass-spring system and two-dimensional FEM. Shear vibrations of the ground can be expressed with this model along with which wave motions propagated through the ground in planar form can be expressed. Comparisons between the model and experimental results are also described below.

MATHEMATICAL MODEL

A soil column having a unit cross-sectional area as shown in Fig. 1 is considered. The equivalent Young's modulus (EF) when this soil column deforms in the shape of a fundamental shearing vibration mode is determined by the following equation.

$$(EF) = \int_0^H E(z)F(z)dZ \quad (1)$$

$$F(z) = \frac{f(z)}{\int_0^H m(z)f(z)dZ / \int_0^H m(z)dZ} \quad (2)$$

where, Z is depth, $E(z)$ is Young's modulus of ground at depth of Z , $m(z)$ is mass at depth of Z , $f(z)$ is fundamental shearing vibration mode, and H is thickness of surface layer.

Eq. (2) indicates the displacement normalized by average displacement.

Similarly, the average Poisson's ratio for this soil column is calculated by the equation below.

$$V = \frac{\int_0^H f(z)v(z)dZ}{\int_0^H f(z)dZ} \quad (3)$$

where, $v(z)$ is Poisson's ratio of ground at depth of Z .

Equations (1), (2) and (3) are used in computation of the stiffness of the plate elements.

Substitution of Soil Column Element by One-Lumped-Mass-Spring System Soil column elements are made by dividing the ground into the mesh shown in Fig. 2. The cross-sectional shape of a soil column was made rectangular in this case, but it would be the same with a triangular cross section.

Letting a soil column in the region demarcated by the dotted line in the figure vibrate at the fundamental shearing frequency at nodal point i , this is substituted by a one-lumped-mass-spring system which expresses this condition. Equivalent spring K_{ei} , and effective mass M_{ei} are obtained by the following equations with total mass of soil column as M_i , fundamental vibration mode as f_i , and fundamental circular frequency as ω_i :

$$K_{ei} = M_i \omega_i^2 \quad (4)$$

$$M_{ei} = (\text{AREA})_i \frac{\int_0^{H_i} m_i(z) f_i(z) dZ^2}{\int_0^{H_i} m_i(z) f_i^2(z) dZ} \quad (5)$$

$$M_i = \int_{(AREA)} dA \int_0^{H_i} m_i(z) dz$$

Stiffness matrix $[K_e]$ connecting basement and mass point can be made from Eq. (4).

Computation of Plate Elements The respective plate elements for the individual soil-column elements in Fig. 2 are computed. At soil-column element J, the four nodal points are numbered j, j+1, i+1, i, and substitution into plate elements is done determining equivalent Young's modulus and Poisson's ratio by the equations below.

$$E_J = \frac{1}{4} \sum_{\ell=j}^i (EF)_{\ell} \quad (6)$$

$$V_J = \frac{1}{4} \sum_{\ell=j}^i V_{\ell} \quad (7)$$

Using E_J and V_J , stiffness matrix $[K_p]$ connecting mass points can be computed by FEM, provided that the condition is to be that of plane stress.

Since Eqs. (6) and (7) compute average values, in applying them it is necessary for appropriate divisions to be made in order that there will not be excessive differences between the values of the four points.

Equation of Motion The equation of motion is as given below.

$$[M] \begin{Bmatrix} \ddot{X} \\ \ddot{Y} \end{Bmatrix} + [C] \begin{Bmatrix} \dot{X} \\ \dot{Y} \end{Bmatrix} + [K] \begin{Bmatrix} X \\ Y \end{Bmatrix} = -[M_e] \begin{Bmatrix} \ddot{U} \\ \ddot{W} \end{Bmatrix} \quad (8)$$

where, $[M]$: mass matrix with M_i as component

$[C]$: damping matrix

$[K]$: sum of $[K_e]$ and $[K_p]$ in matrix K

$[M_e]$: effective mass matrix

X, Y : displacements of mass points in x and y directions

\ddot{U}, \ddot{W} : accelerations of basement in x and y directions

Since the displacements of the various mass points, in effect, the average displacements of the ground at the individual nodal points are determined by solving this equation, the distribution of displacements in the direction of depth can be computed by Eq. (2). The reasons earthquake response in the vertical direction was not included were that the response displacement in the vertical direction is small compared with the horizontal direction, and that it was aimed to reduce the scale of calculations in consideration of practicality. However, in computation of the matrix $[K_p]$ obtained from plate elements, since a plane stress state is assumed, vertical displacement accompanying earthquake response in the horizontal direction is computed from these calculations.

MODEL VIBRATION EXPERIMENTS

A soft surface layer ground model was made on a shaking table to verify the appropriateness of the mathematical model described in the preceding section and resonant vibration experiments were conducted. The model ground was made under especially severe conditions in order to investigate whether this mathematical model would adequately express the dynamic behavior of the ground.

Fig. 4 is a plan of a model alluvial ground, the contour lines being those of the basement in units of centimeters. The basement was made of plaster, while acrylic amide gel was used for the alluvial ground, and since contour lines were provided to 0, the thickness of the alluvial layer was as much as 20 m at the upper valley part. It can be seen that the slopes of the valley are very steep at the left and lower valley sides. The boundaries at the upper valley part and

the lower valley right side are free boundaries.

The shear wave velocity of the alluvial layer is 240 cm/sec, which is extremely low compared with that of the basement so that natural frequency is amplified at the surface layer. The Poisson's ratio is estimated to be approximately 0.499, and since the propagation velocity of compression waves is extremely high compared with the velocity of shear waves, a distinct separation between shear waves and compression waves is made, and in the frequency range of the experiments, it is practically only shear waves that are predominant.

The straight lines intersecting in grid form in Fig. 4 are thin rubber strings buried in the surface layer portion, and are for measuring and observing the vibration mode of the surface. A multiple number of miniature accelerographs are installed at the shaking table and the surface for observations of frequencies, amplitudes, and phases. Furthermore, the vibrating conditions of the surface were recorded by photographs also.

The experiments were conducted rotating the exciting direction 15 deg at a time. Figs. 5 to 7 show low-order predominant vibrations determined from amplitudes and phases of vibrations at the surface. Although the fundamental vibrations are seen very distinctly, at higher than the third order it is difficult to obtain a vibration condition with a constant phase over the entire model, and it is not an easy matter to establish the frequency and mode. This is thought to be in part because of being influenced by the damping ratio of the material of approximately 1 percent. The fundamental vibration mode occurs in a very stable manner, and this appears if there is the slightest component of excitation in the axial direction of the valley.

Next, on dividing into an element mesh like the grid in Fig. 4, the natural vibrations of the surface layer are calculated by Eq. (9) using the method described under "Mathematical Model," and the natural vibration modes are shown in Figs. 8 through 12.

$$[K]\begin{Bmatrix} X \\ Y \end{Bmatrix} = \omega^2 [M]\begin{Bmatrix} X \\ Y \end{Bmatrix} \quad (9)$$

COMPARISONS OF EXPERIMENTAL AND ANALYTICAL RESULTS

On comparisons of experimental and analytical results, it can be seen that there is very good agreement between the predominant vibration at the lowest frequency and the fundamental vibration. In Figs. 9 and 10 the modes are fairly similar, the frequencies being close together at 4.24 Hz and 4.31 Hz, respectively. The second-order mode in the experimental results can be seen to be intermediate among these modes. The third-order mode in the experimental results correlate with the fifth-order mode in the analytical results. The fourth-order mode in the analyses was not recognized in the experiments. Thereupon, correlating the natural (predominant) vibrations of similar modes in the experiments and analyses, the frequencies will be as tabulated below.

Table Natural (Predominant) Frequencies from Experiments and Analyses

Mode No.	Predominant Frequency from Experiments (Hz)	Natural Frequency from Analyses (Hz)
1	3.64	3.72
2	4.40	4.24
3	4.94	4.60

Although it may be considered that the method of division had also affected the analytical results, the foregoing results may be evaluated as giving good agreement between analyses and experiments in the low-order predominant vibration region in spite of the various factors previously mentioned. That low-order predominant vibrations of the surface layer are generated predominantly, and that the low-order amplitudes are relatively large indicate how significant this model is.

In closing, the authors wish to express their gratitude to Mr. M. Inamori of the Institute of Construction Technology, Kumagai-Gumi Co., Ltd., for his invaluable cooperation in conducting the experiments for this study.

References

A quasi-three-dimensional ground model for earthquake response analysis of underground structures — Construction of ground model — ; Choshiro Tamura and Takeyasu Suzuki, SEISAN KENKYU, Vol.39, No.1, Jan., 1987
 A quasi-three-dimensional ground model for earthquake response analysis of underground structures — Verification of the model by vibration tests — ; Takeyasu Suzuki, Mitsuhiro Inamori and Choshiro Tamura, SEISAN KENKYU, Vol. 39, No.2, Feb., 1987

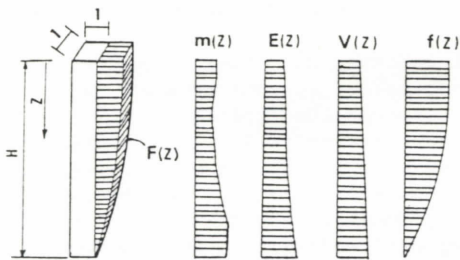


Fig. 1 Equivalent Young's Modulus (EF) and Poisson's Ratio

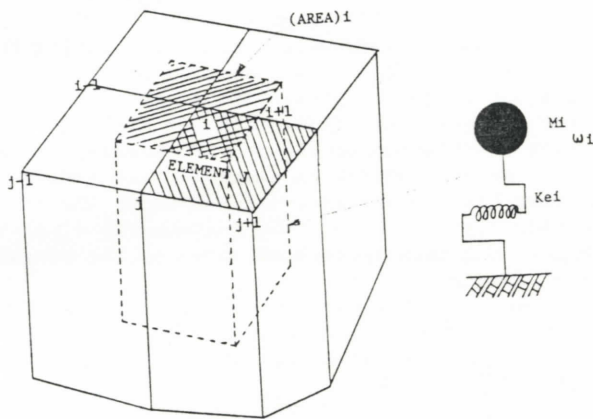
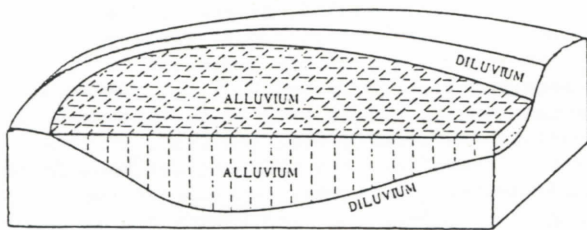
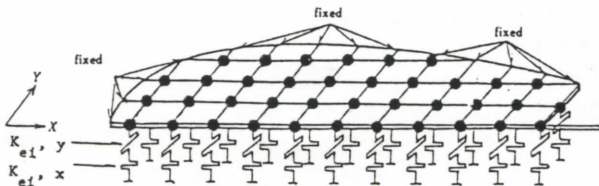


Fig. 2 One-Lumped-Mass-Spring System Representation



(a) Modeled Ground Profile



(b) Model of Alluvial Layer

Fig. 3 A Schematic Representation of the Proposed Method to Modelize Alluvial Ground

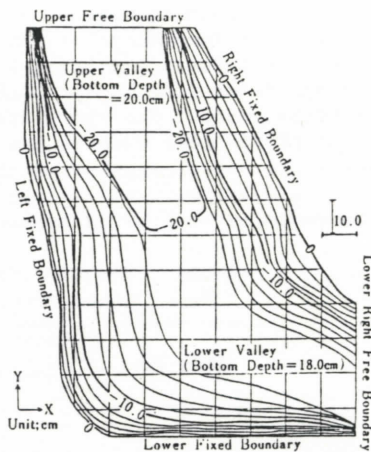


Fig. 4 Plan of Alluvial Layer of a Experimental Ground Model

Frequency : 3.64 Hz

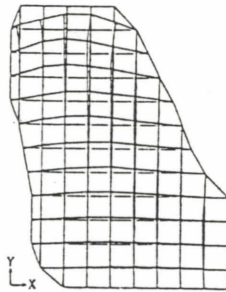


Fig. 5 Lowest Predominant Mode of the Experiment

Frequency : 4.40 Hz

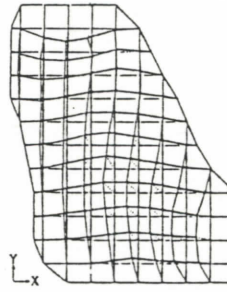


Fig. 6 Second Predominant Mode of the Experiment

Frequency : 4.94 Hz

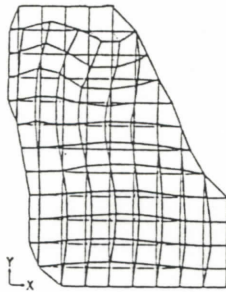


Fig. 7 Third Predominant Mode of the Experiment

Frequency : 3.72659 Hz
Participation Factor : 0.13998

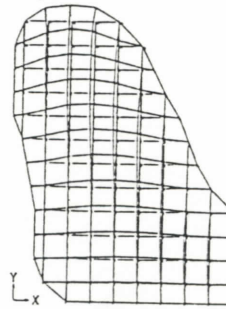


Fig. 8 Fundamental Natural Mode of the Analysis

Frequency : 4.24109 Hz
Participation Factor : 0.35030

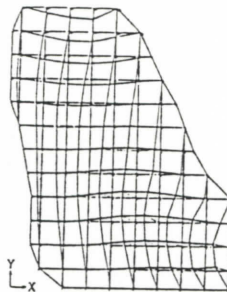


Fig. 9 Second Natural Mode of the Analysis

Frequency : 4.30932 Hz
Participation Factor : 0.11880

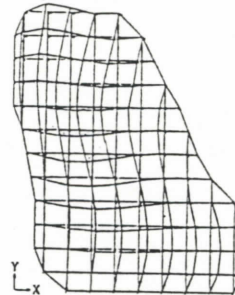


Fig. 10 Third Natural Mode of the Analysis

Frequency : 4.37482 Hz
Participation Factor : 0.01807

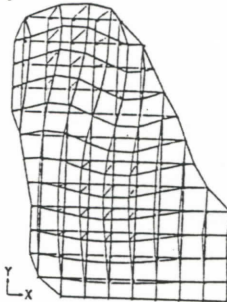


Fig. 11 Fourth Natural Mode of the Analysis

Frequency : 4.59969 Hz
Participation Factor : 0.21212

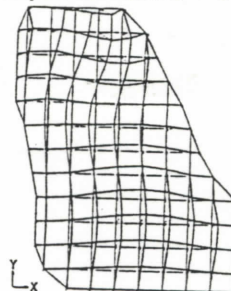


Fig. 12 Fifth Natural Mode of the Analysis